Ultrafast Dynamics of Liquid Water and Ice

Fivos Perakis[§] and Peter Hamm*

[§]SCS-DSM Award for best poster presentation

Abstract: In the present contribution we summarize our observations concerning the ultrafast non-equilibrium dynamics of water, in both the liquid and crystalline phase. Our experimental tool is two-dimensional infrared (2D IR) spectroscopy, which combines structural information on a molecular level with femtosecond time resolution. In the case of liquid and supercooled water we are able to extract the timescales of hydrogen bonding dynamics, whereas in the ice form we can probe the change of the hydrogen bond properties under excitation and observe the influence of intermolecular mode excitations in the crystal.

Keywords: Ice Ih · 2D IR spectroscopy · Supercooled water · Time-resolved vibrational spectroscopy

Introduction

From a physico-chemical point of view, liquid water reveals surprisingly uncommon features.[1] Its thermodynamic properties deviate from that of common liquids,[2] and from a microscopic point of view the structure of liquid water is still under debate.[3] By structure of course we do not mean the structure of the individual water molecule, but that of the molecular network held together by hydrogen bonds. The commonly accepted picture features tetrahedral h-bond motives (*i.e.* each molecule bounded in average to four others), which locally are structurally similar to ice.[4] Ice, the crystalline phase of water, has been extensively studied and its phase diagram has been extended to include up to 15 different forms.[5] Ice Ih is the form of all natural snow and ice on Earth, which has hexagonal structure with respect to the oxygen positions, whereas it is disordered with respect to the hydrogens (proton disorder).

However crystallization (freezing resulting to ice) is only one of the possibilities. If the liquid is free from impurities, water can be *supercooled* (*i.e.* cooled and remain in the liquid phase) down to T_H = –38° C at 1 bar.[6] This limit is known as the *homogeneous nucleation limit*, as liquid water freezes spontaneously below T_H. Interestingly, many thermodynamical quantities extrapolated below this limit, become infinite for the *singular temperature* T_S = –45 °C.[7] This singular temperature is connected with the debate concerning the transition of liquid water to a glass.[8] Glassy water (solid but with liquid-like molecular structure), also called amorphous ice, is believed to be a continuous extension of the liquid phase. According to this hypothesis, the hydrogen bonding exchange of liquid water should slow down by cooling, until a critical temperature where it completely stops, resulting in the glass phase.[8]

Our experiments discussed here monitor the h-bonding exchange rate as a function of temperature, which indeed slows down,[9] in agreement with literature.[10,11] Additionally we discuss the relation of experimental data of liquid water with that of ice Ih,[12] trying to elucidate possible dynamic and structural similarities between the two.

Two-dimensional Infrared Spectroscopy

Two-dimensional infrared (2D IR) spectroscopy is a powerful technique applied in a very broad variety of systems, due to its ability to access bond specific structural information with ultrafast time resolution.[13,14] The tools at our disposal are ultrashort laser pulses (70 fs = 70 · 10^{-15} seconds), centered in the mid-infrared (λ = 3–10 μm) which allow us to induce and

Correspondence: Prof. Dr. P. Hamm
University of Zurich
Institute of Physical Chemistry
Winterthurerstr. 190
CH-8057 Zurich
Tel.: +41 44 635 44 31
Fax: +41 44 635 68 38
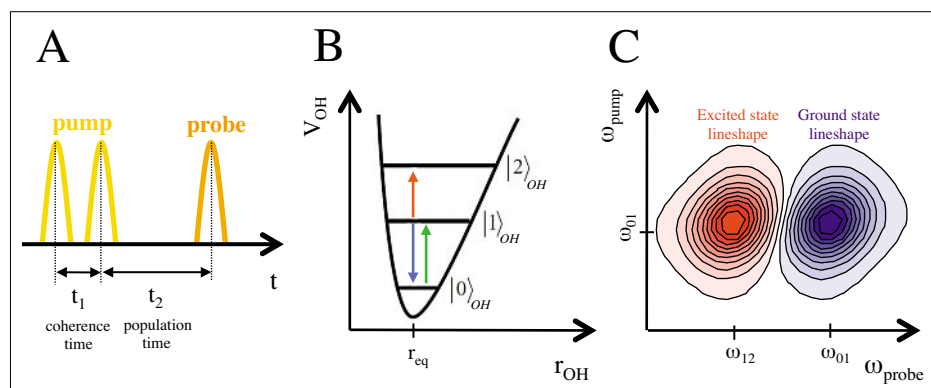E-mail: phamm@pci.uzh.ch

Fig. 1. (A) The pulse sequence of the experiment, (B) the way the probe pulse interacts with the sample, as described on the electronic potential between oxygen and hydrogen and (C) the resulting 2D IR spectra.

observe vibrational molecular excitations. Fig. 1A shows a scheme of the laser pulses sequence used in 2D IR spectroscopy.[15] The first two pulses initiate the vibration (pump pulses) whereas a subsequent pulse (probe pulse) allows us to monitor the evolution of the excitation. The time between the two pump pulses is called the *coherence time* t_1, and by measuring the interference of these two pulses we can generate the corresponding frequency axis ω_{pump} by a Fourier transformation (vertical axis in Fig. 1C). The time between pump and probe pulses, referred to as *population time* t_2, is the time we give the system to evolve between exciting the vibration (pump) and monitoring it (probe).

In Fig. 1B we illustrate the way light interacts with the sample. Here is shown schematically the electronic ground state potential between the oxygen and the hydrogen as a function of the distance between them r_{OH}. $|0\rangle_{OH}$, $|1\rangle_{OH}$ and $|2\rangle_{OH}$ are the corresponding vibrational eigenstates. The first pump pulse excites a certain fraction of the molecules from the equilibrium ground state to the first vibrational excited state $(|0\rangle_{OH} \rightarrow |1\rangle_{OH})$. Consequently the probe pulse can (i) excite the already excited molecules to a higher excited state $|2\rangle_{OH}$ (red arrow – excited state absorption), (ii) de-excite the molecules back to the ground state (blue solid arrow – stimulated emission) or (iii) excite some of the remaining ground state molecules to the first excited state $|1\rangle_{OH}$ (green arrow – bleaching). Because the potential is anharmonic, the frequency ω_{12} needed for the transition $|1\rangle_{OH} \rightarrow |2\rangle_{OH}$ (red arrow) is less than ω_{01} needed for the $|0\rangle_{OH} \rightarrow |1\rangle_{OH}$ (blue arrow). In Fig. 1C is shown the resulting two-dimensional infrared (2D IR) spectra, obtained by plotting the frequency of the pump ω_{pump} as a function of the probe ω_{probe}. These spectra result from the difference of the signal between the case when the sample is pumped minus when it is not. The result is two lobes with opposite signs, as

indicated by the color code. The blue lobe in Fig. 1C is associated with ground state processes (blue and green arrows in Fig. 1B), as can be seen from the frequency: in both pump and probe axes is ω_{01}. The corresponding red lobe is associated with excited state processes (red arrow in Fig. 1B), as its frequency is ω_{01} along the pump axis and ω_{12} along the probe. Both lobes constitute the 2D IR signal, the shape and dynamics of which can reveal information associated with the molecular interactions of the system.[14] In liquid water for example, we can learn about the hydrogen bond exchange rate, and how this changes with temperature, as discussed in the next section.

Liquid and Supercooled Water

The OH stretch vibrational mode of liquid water is a direct probe of the underlying hydrogen bonding environment. A free water molecule (not h-bonded) is expected to have slightly different frequency than one that is h-bonded with another. In other words, at each instant of time the local environment of each water molecule is different, resulting in slightly different frequencies and rendering the OH stretch band *inhomogeneously broadened*. Such an example is shown in Fig. 2A as a scheme of an inhomogeneously broadened band (black line) with the various contributions corresponding to the hypothetical different environments (colored lines). The 1D experiment (FTIR) can only resolve the overall lineshape (black line) without providing any information about the underlying inhomogeneity (colored lines).

Using 2D IR spectroscopy, we can monitor the change in hydrogen bonding,[16–19] *i.e.* how the various local environments reorganize between pump and probe excitations (during t_2). Imagine that we can monitor the frequency of one of these O-H oscillator populations (upper

row in Fig. 2B). If the pump and probe pulses arrive simultaneously ($t_2 = 0$ fs) the water molecule has not changed h-bond partners and its frequency is still the same. The corresponding 2D IR response would then reveal the same frequency for both axes. Generalizing this for all the underlying contributions, all the different structural motives would have the same frequency for both pump and probe axes, making the 2D IR lineshape *diagonally elongated* (left 2D IR spectrum in Fig. 2B). Allowing the system a bit of time to evolve ($t_2 = 500$ fs) the water clusters change h-bond partners and structurally rearrange, resulting to a frequency shift (upper row in Fig. 2B). Because of this shift, the correlation between the pump and probe frequency will be reduced, which makes the 2D IR lineshape rounder and less tilted (right 2D IR spectrum in Fig. 2B). By measuring the slope of the ground state lineshape (*i.e.* the tilt), as a function of population time t_2, we can measure the characteristic timescales of the hydrogen bond exchange dynamics. This is often referred to as *spectral diffusion* and is associated with the memory of the system.[14]

The experimental data of the OD stretch of HOD in H_2O for different population times ($t_2 = 50, 500$ and 1000 fs) are presented at Fig. 3A. The upper row corresponds to spectra taken at 290 K, whereas the lower one to that of supercooled water at 260 K. In green is shown the calculated central slope, the relative value of which relates to the correlation decay between pump and probe. It is evident that correlation decays much faster for the liquid at ambient conditions (Fig. 3A upper row) than in the case of supercooled water (Fig. 3A lower row), which even for later times exhibits a tilt. This means that h-bonding exchanges faster in the stable liquid than in supercooled water.

To quantify the hydrogen bonding exchange rate, we extract the value of the central slope from each 2D IR spectrum and plot it as a function of population time (Fig. 3B). Mono-exponential fits (solid lines) capture the characteristic timescale of the decay, indicating that h-bonding exchange happens for ambient conditions at 0.7 ps, whereas for supercooled water slows down to 2.6 ps. Extension of these measurements to different temperatures suggests that h-bonding rate exhibits power law temperature dependence (indicative of a glass forming liquid[8]), with a singular temperature at 221 K, in agreement with other experimental values.[10,11]

Ice Ih

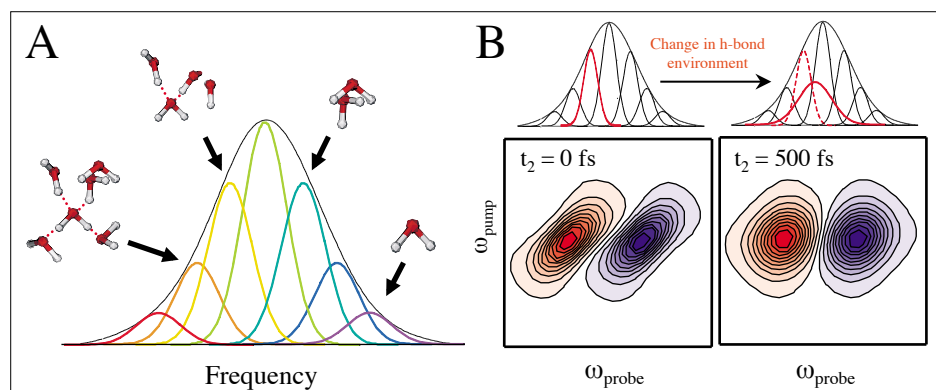Interesting conclusions stem from the comparison of the liquid water 2D line-

Fig. 2. (A) The various hydrogen bonding motives correspond to different frequencies, underlying the OD stretch mode. (B) A change in a local h-bonding environment results to a change in frequency. This does not affect the shape of the 1D spectrum (upper row), whereas it is evident in the 2D IR spectrum by making the lineshape more round (lower row).
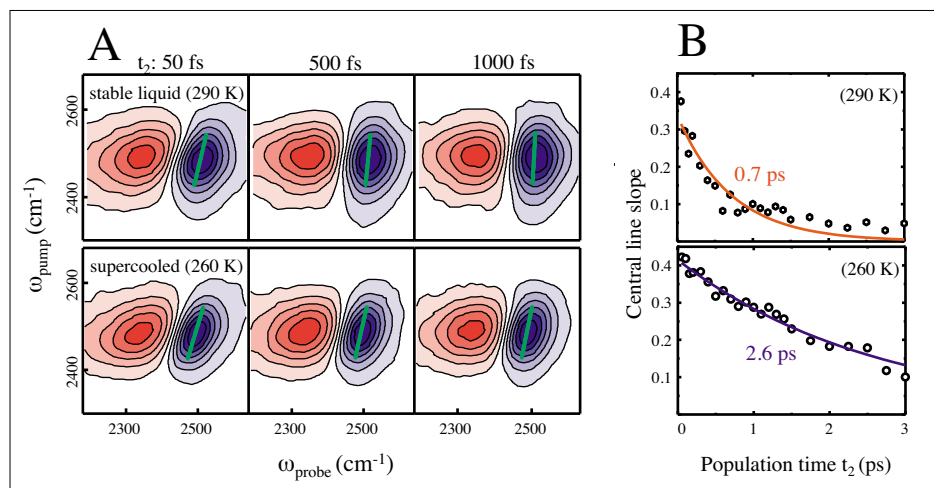
Fig. 3. (A) Experimental data of the OD stretch vibration of HOD in H_2O, for different population times and temperatures. As can be seen from the central slope of the ground state lineshape (green line) the correlation between pump and probe decays much faster for the stable liquid than for supercooled water. (B) The value of the central slope for different population times. The exponential fits (solid lines) reveal that the h-bonding exchange occurs with a time constant of 0.7 ps for stable liquid and 2.6 ps for supercooled water (figure adapted from ref. [9]).

shape with that of ice. In Fig. 4B are shown the 1D absorbance spectrum of the OD stretch of ice Ih (solid line) and of liquid water (dashed line). The lineshape of ice is much narrower than that of liquid water. That is due to the fact that water molecules in ice are ordered in a crystal lattice (Fig. 4A right), and the variety of structural motives (inhomogeneity) is much less than that of liquid water (Fig. 4A left). Also the ice band appears shifted to lower frequencies which is a result of stronger hydrogen bonds.

Interestingly the 2D IR spectrum of ice (Fig. 4C) exhibits a very broad excited state lineshape (red lobe), which has been observed before by pump-probe measurements.[20,21] This feature is very uncommon in 2D IR spectroscopy, as typically the ground and excited state 2D lineshapes are of comparable amplitude and shape. A similar feature can be seen to some extent for liquid water (Fig. 3A) which however is less pronounced due to the inhomogeneity of the liquid. Overall the lineshape does not exhibit any diagonal elongation (like that of water discussed in Fig. 2), another evidence of the homogeneous environment of ice and the absence of any hydrogen bond dynamics on the observed timescales.

To understand the origin of the broad excited state lineshape we perform quantum-dynamical simulations, using the Lippincott-Schroeder (LS) potential. The LS model is a phenomenological potential developed for hydrogen-bonded crystals,[22] and has been previously applied to liquid water and ice.[21,23] The potential describes the interaction between two water molecules as a function of the *intramolecular distance* r_{OH} between the oxygen and the covalently bonded hydrogen and

the *intermolecular distance* $R_{O\cdots O}$ between the two oxygens as indicated in Fig. 5A. Plotting the LS potential as a function of the O-H distance (for a fixed $R_{O\cdots O} = 2.76$ Å) results in two minima (Fig. 5B). The deeper one ($r_{OH} = 1$ Å) describes the situation when the proton involved in the hydrogen bond is covalently bound to the donating water ($H_2O + H_2O$), whereas the other minimum ($r_{OH} = 1.7$ Å) corresponds to the case where the proton is transferred, forming a $OH^- + H_3O$ pair. The double-minimum feature renders this potential a

more sophisticated and realistic version of the one discussed in the Fig. 2B. The states $|0\rangle_{OH}$, $|1\rangle_{OH}$ and $|2\rangle_{OH}$ are the corresponding vibrational states, which can be acquired by solving the *nuclear Schrödinger equation* for the LS potential.

Just like in the Born-Oppenheimer approximation, where one assumes that the nuclear degrees of freedom can be adiabatically separated from the electronic degrees of freedom, one may make a similar adiabatic approximation, separating the fast O-H motion from the ten times slower O···O motion. Fig. 5C shows the dependence of the O-H vibrational energy of states $|0\rangle_{OH}$, $|1\rangle_{OH}$ and $|2\rangle_{OH}$ on the intermolecular distance $R_{O\cdots O}$. When subsequently quantizing the O···O motion, we end up with a picture that is formally equivalent to Franck-Condon transitions in electronic spectroscopy. Note however that all this is happening on the electronic ground state surface. In other words, Franck-Condon like progressions are obtained for the $|0\rangle_{OH} \rightarrow |1\rangle_{OH}$ and the $|1\rangle_{OH} \rightarrow |2\rangle_{OH}$ transitions (as indicated by the arrows in Fig. 5C), that are another mechanism for line broadening. The details of the LS potential reveal a more pronounced Franck-Condon progression for the $|1\rangle_{OH} \rightarrow |2\rangle_{OH}$ than for the $|0\rangle_{OH} \rightarrow |1\rangle_{OH}$ transition, and qualitatively reproduce the experimentally observed asymmetry of the 2D lineshape (see Fig. 4C,D).[12] It is important to note that this line-broadening mechanisms directly reflects the very strong and very specific anharmonic coupling between the O-H and
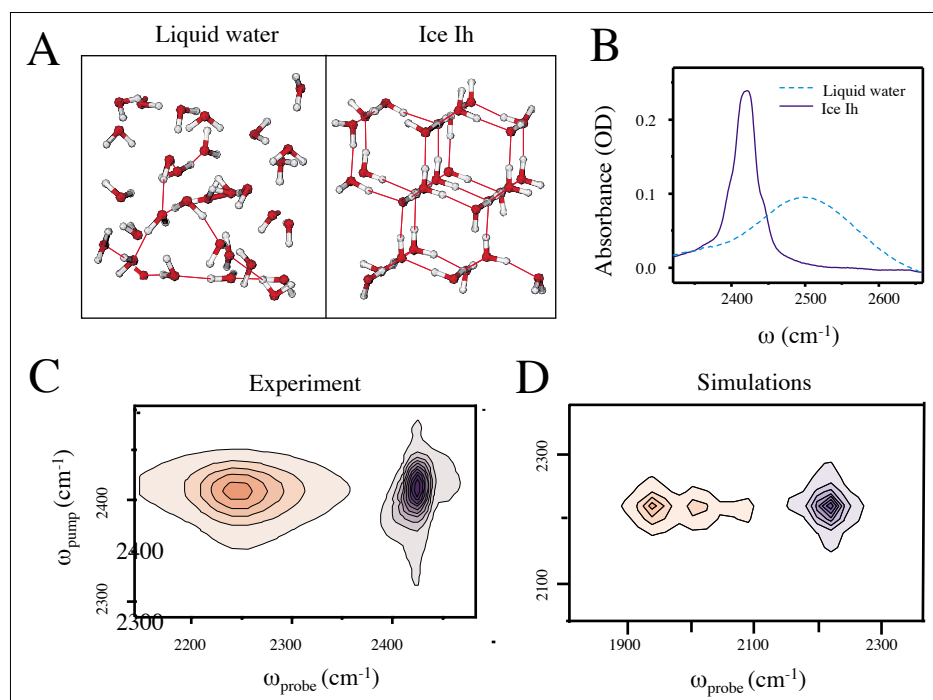

Fig. 4 (A) Comparison of the inhomogeneous environment of liquid water (left) with the more ordered case of ice Ih (right). (B) The 1D absorbance spectrum the OD stretch vibration of HOD in H_2O of ice Ih (solid line) and liquid water (dashed line). (C) Experiment and (D) simulation 2D IR spectra of the OD stretch vibration of ice Ih (figure adapted from ref. [12])
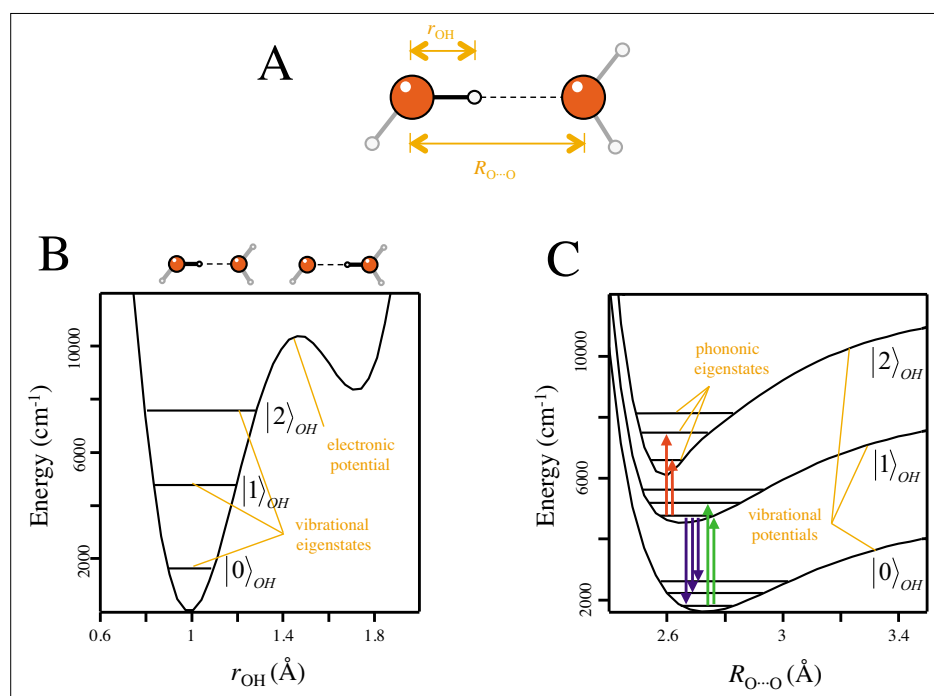
Fig. 5 (A) The LS model describe the interaction between two water molecules as a function of the distance r_{OH} and $R_{O\cdots O}$. (B) The electronic potential as a function of the r_{OH} and the corresponding OH-vibrational eigenstates. (C) The adiabatic vibrational potentials for the various OH states as a function of the $R_{O\cdots O}$ and the corresponding O$\cdots$O eigenstates. (figure adapted from ref. [12])

the O$\cdots$O degrees of freedom, and that 2D IR spectroscopy is explicitly sensitive to molecular anharmonicity (as one can show on very general grounds that the 2D IR response of perfectly harmonic states would vanish).

Conclusions

In the current contribution, we summarize our results on the 2D IR spectroscopy of water in its various states. In the case of liquid water, we are able to extract the timescales of hydrogen bonding and how this changes as a function of temperature from ambient conditions (0.7 ps) down to the supercooled regime (2.6 ps).[9] Comparison of the liquid lineshape with that of ice Ih reveals that hydrogen bonding in water is a highly anharmonic interaction with respect to intramolecular as well as the intermolecular degrees of freedom.[12] Subsequent 2D IR investigations on neat ice Ih (and not isotope diluted) investigate the origin of the multiple peaks in the 1D spectra, probing the excitonic coupling of the system which results to very fast dipole randomization.[24]

[1] F. Franks, 'Water: a matrix of life', Royal Society of Chemistry, Great Britain, **2000**.
[2] P. G. Debenedetti, *J. Phys.: Condens. Matter* **2003**, *15*, R1669.
[3] R. Ludwig, *Angew. Chem. Int. Ed.* **2001**, *40*, 1808.
[4] P. Ball, *Nature* **2008**, *452*, 291.
[5] E. A. Zheligovskaya, G. G. Malenkov, *Russ. Chem. Rev.* **2006**, *75*, 57.
[6] C. A. Angell, *Annu. Rev. Phys. Chem.* **1983**, *34*, 593.
[7] O. Mishima, H. E. Stanley, *Nature* **1998**, *396*, 329.
[8] P. G. Debenedetti, F. H. Stillinger, *Nature* **2001**, *410*, 259.
[9] F. Perakis, P. Hamm, *J. Phys. Chem. B* **2011**, *115*, 5289.
[10] R. Torre, P. Bartolini, R. Righini, *Nature* **2004**, *428*, 296.
[11] R. A. Nicodemus, K. Ramasesha, S. T. Roberts, A. Tokmakoff, *J. Phys. Chem. Lett.* **2010**, *1*, 1068.
[12] F. Perakis, S. Widmer, P. Hamm, *J. Chem. Phys.* **2011**, *134*, 204505.
[13] P. Hamm, *Chimia* **2011**, *65*, 313.
[14] P. Hamm, M. Zanni, 'Concepts and Methods of 2D Infrared Spectroscopy', Cambridge University Press, **2011**.
[15] J. Helbing, P. Hamm, *J. Opt. Soc. Am. B* **2011**, *28*, 171.
[16] M. L. Cowan, B. D. Bruner, N. Huse, J. R. Dwyer, B. Chugh, E. T. J. Nibbering, T. Elsaesser, R. J. D. Miller, *Nature* **2005**, *434*, 199.
[17] J. B. Asbury, T. Steinel, C. Stromberg, S. A. Corcelli, C. P. Lawrence, J. L. Skinner, M. D. Fayer, *J. Phys. Chem. A* **2004**, *108*, 1107.
[18] J. D. Eaves, J. J. Loparo, C. J. Fecko, S. T. Roberts, A. Tokmakoff, P. L. Geissler, *PNAS* **2005**, *102*, 13019.
[19] S. Yeremenko, M. S. Pshenichnikov, D. A. Wiersma, *Chem. Phys. Let.* **2003**, *369*, 107.
[20] G. Seifert, K. Weidlich, H. Graener, *Phys. Rev. B* **1997**, *56*, R14231.
[21] A. M. Dokter, H. J. Bakker, *J. Chem. Phys.* **2008**, *128*, 024502.
[22] E. R. Lippincott, R. Schroeder, *J. Chem. Phys.* **1955**, *23*, 1099.
[23] H. J. Bakker, H.-K. Nienhuys, *Science* **2002**, *297*, 587.
[24] F. Perakis, P. Hamm, *Phys. Chem. Chem. Phys.* **2011**, DOI 10.1039/C2CP23710E.